# Accurate, smooth, local, energy-dependent optical potentials for electron scattering

David W. Schwenke, Devarajan Thirumalai, and Donald G. Truhlar
*Department of Chemistry, University of Minnesota, Minneapolis, Minnesota 55455*
(Received 21 June 1983)

We present a new method for obtaining local, energy-dependent, single-channel or multichannel optical potentials. The optical potential is obtained by calculating and smoothing a potential that yields the correct scattering matrix for a sequence of truncated interaction-potential matrices. The new method is illustrated by applications to electron—hydrogen-atom scattering in a truncated Hilbert space. The resulting optical potentials accurately reproduce the original close-coupling calculations in the same Hilbert space, and they show clearly the effects of charge polarization and flux absorption. The coordinate dependence and energy dependence of the smoothed optical potentials are compared to models in the literature.

## I. INTRODUCTION

The inclusion of virtual and real charge-polarization effects is the hardest part of electron scattering theory and the most difficult effect to include in computations. The three most standard approaches are (i) inclusion of a sufficient number of excited electronic states or pseudostates of the target in a coupled-channel treatment of the dynamics,[1-4] (ii) calculation of a nonlocal optical potential by Green's-function theory, perturbation theory, or the Feshbach projection-operator formalism,[5-15] (iii) use of local, energy-dependent effective potentials obtained by high-energy, low-energy, or semiclassical approximations, or from models.[16-32] Approaches (i) and (ii) are more rigorous than (iii), but they are expensive to converge and not as easily interpreted as approach (iii). In approach (iii) the real part of the optical potential is usually based on a static-exchange potential plus a "polarization" term based on the adiabatic approximation, with or without nonadiabatic corrections. In phenomenological models, the polarization potential contains an empirical parameter adjusted to experimental scattering data,[33-35] but this is not necessary.[16-31] The imaginary part, or "absorption" term, is harder to model and is often based on simply motivated functional forms with empirical parameters.[36,37] The eikonal optical model,[22] the dispersion relation for the absorption potential,[38] and a quasifree scattering model[32] have also been used to obtain the imaginary part of the optical potential without empirical parameters, and the dispersion relation has also been used with empirical imaginary parts to obtain the form of the polarization part.[39] These methods have their merits, but it is still not completely clear which forms are best for the polarization and absorption terms in the optical potential.

A fourth approach that does not fit into the above classification is (iv) the matrix effective-potential method.[28,40] This method may be thought of as an attempt to bridge classes (i) and (iii) since it is a coupled-channels method, but the input is obtained from an adiabatic model rather than from excited-state or pseudostate wave functions. The final results of the matrix effective-potential method show energy-dependent nonadiabatic polarization effects implicitly.

The single-channel effective-potential approaches and the optical-potential approach can be cast in a unified notation by defining the optical potential as

$$V^{\rm opt}(\vec{r}) \equiv V_{11}^{SE}(\vec{r}) + Q_{11}(\vec{r}) , \tag{1}$$

where $V_{11}^{SE}(\vec{r})$ is the first element of the static-exchange potential matrix, $\vec{r}$ is the coordinate of the scattering particle, and $Q_{11}(\vec{r})$ is an optical-correction potential. Comparing this to the usual effective-potential notation

$$V^{\rm eff}(\vec{r}) = V_{11}^{SE}(\vec{r}) + V^{P}(\vec{r}) + iV^{A}(\vec{r}) , \tag{2}$$

where $V^{P}(\vec{r})$ is the polarization potential and $V^{A}(\vec{r})$ is the absorption potential, shows that

$$Q_{11}(\vec{r}) = V^{P}(\vec{r}) + iV^{A}(\vec{r}) . \tag{3}$$

Note that every term in Eqs. (1)—(3) is also a function of energy. In this article we will also consider $n \times n$ generalized-optical-potential matrices $\underline{V}^{\rm opt}(\vec{r})$, in which case $V^{\rm opt}(\vec{r})$ is $V_{11}^{\rm opt}(\vec{r})$.

One way to illustrate the relationship between the approaches and to use approaches of class (i) to gain more insight about the terms in Eq. (3) is to use approach (i) for tractable cases and find numerically exact local optical potentials that reproduce submatrices of the scattering matrix of the full calculations for a given energy.[41] We have tried this, and, as we show in this paper, the resulting numerical optical potentials contain many poles, and they are not easy to interpret. The method would be more useful if we could obtain smooth, local optical potentials that still reproduce or almost reproduce the results of the full calculation. We will show in this paper that this can be achieved by smoothing the original numerical optical potentials. Our procedures yield a local, energy-dependent, smoothed optical potential that is essentially exact. We hope that this kind of potential, which contains no semiempirical parameters and which presupposes no functional form, will be useful for illustrating the features that a physically correct model potential should have.

In this paper we give all numerical values in Hartree atomic units, in which the energy unit is 1 hartree

 

$=1E_h=27.2116$ eV$=4.359\,81\times10^{-18}$ J, and the length unit is 1 bohr $=1a_0=0.529\,177$ Å.

## II. EXAMPLE

All numerical examples in this article are for electron–hydrogen-atom scattering with zero total angular momentum and neglecting exchange. Higher angular momenta and inclusion of exchange will have quantitative effects on the results, but the example considered here is sufficient to illustrate the new method and the energy dependence of the optical potential. We expand the scattering wave function in terms of five eigenstates and pseudostates of the target: $1s$, $2s$, $\overline{2p}$, $\overline{3s}$, and $\overline{3d}$. For total angular momentum zero, there is one channel per state, and we will use these state designations as the channel indices. The pseudostates $\overline{2p}$ and $\overline{3d}$ are those of Temkin,[42] and Damburg and Karule,[43] and, respectively, they take full account of the long-range dipole and quadrupole polarizabilities of the ground state. The $\overline{3s}$ state was taken from Burke and Mitchell,[44] and it accounts for short-range radial correlation effects. The radial parts and eigenvalues of the eigenstates and pseudostates are given in Table I. The last column of Table I gives the threshold energies.

TABLE I. Radial parts and eigenvalues of the eigenstates and pseudostates used in the close-coupling calculations.

| State | $R_\alpha(r)$[a] | $E_a^0$ ($E_h$) | $(E_a^0-E_1^0)$ ($E_h$) |
|---|---|---|---|
| $1s$ | $2e^{-r}$ | $-\frac{1}{2}$ | 0.000 00 |
| $2s$ | $(\frac{1}{2})^{1/2}(1-\frac{1}{2}r)e^{-r/2}$ | $-\frac{1}{8}$ | 0.375 00 |
| $\overline{2p}$ | $(\frac{32}{129})^{1/2}r(1+\frac{1}{2}r)e^{-r}$ | $-\frac{7}{86}$ | 0.418 60 |
| $\overline{3s}$ | $[(\frac{300}{152})^{1/2}-(\frac{529}{456})^{1/2}r+(\frac{3}{152})^{1/2}r^2]e^{-r/2}$ | $-\frac{5}{456}$ | 0.489 04 |
| $\overline{3d}$ | $(\frac{32}{535})^{1/2}r^2(\frac{1}{2}+r/3)e^{-r}$ | $+\frac{13}{214}$ | 0.560 75 |

[a]In atomic units. The normalization is $\int_0^\infty dr\, r^2\,|R_\alpha(r)|^2=1$.

## III. METHODS

The construction of the optical potential involves three steps. First, it is necessary to solve the many-channel close-coupling equations for the scattering wave function. The next step is the calculation of the exact optical potential using the method of Wolken.[41] Finally, the exact optical potential is smoothed to remove its poles.

We consider electron-atom scattering, neglecting exchange. The close-coupling equations for total angular momentum zero are

$$\left[\frac{d^2}{dr^2}-\frac{l_\alpha(l_\alpha+1)}{r^2}+k_\alpha^2\right]f_{\alpha\alpha_0}(r)=\frac{2\mu}{\hbar^2}\sum_{\alpha'}V^S_{\alpha\alpha'}(r)f_{\alpha'\alpha_0}(r),\quad \alpha,\alpha'=1,\ldots,N \tag{4a}$$

$$k_\alpha^2=(2\mu/\hbar^2)E_{\mathrm{rel},\alpha}\ , \tag{4b}$$

$$E_{\mathrm{rel},\alpha}=E-E_\alpha^0\ , \tag{4c}$$

$$\begin{aligned}V^S_{\alpha\alpha'}(r)=&\sum_{m_l=-l_\alpha}^{l_\alpha}\sum_{m_l'=-l_{\alpha'}}^{l_{\alpha'}}\sum_{m_j=-j_\alpha}^{j_\alpha}\sum_{m_j'=-j_{\alpha'}}^{j_{\alpha'}}(l_\alpha m_l j_\alpha m_j\,|\,l_\alpha j_\alpha 00)(l_{\alpha'}m_l' j_{\alpha'}m_j'\,|\,l_{\alpha'}j_{\alpha'}00)\\&\times\int d\vec{r}\,'\,d\hat{r}\,Y^*_{l_\alpha m_l}(\hat{r})Y^*_{j_\alpha m_j}(\hat{r}')R_{n_\alpha l_\alpha}(r')\left[\frac{e^2}{|\vec{r}\,'-\vec{r}\,|}-\frac{e^2}{r}\right]\\&\times Y_{l_{\alpha'}m_l'}(\hat{r})Y_{j_{\alpha'}m_j'}(\hat{r}')R_{n_{\alpha'}l_{\alpha'}}(r')\ ,\end{aligned} \tag{4d}$$

where $l_\alpha$ is the orbital angular quantum number of relative motion in channel $\alpha$, $n_\alpha$ and $j_\alpha$ are principal and orbital quantum numbers of internal motion in channel $\alpha$, $(\cdots\,|\,\cdots)$ is a Clebsch-Gordan coefficient,[45] $Y_{lm}$ is a spherical harmonic,[45] $\mu$ is the reduced mass, $E$ is the total energy, $\alpha_0$ specifies the boundary conditions, $E_{\mathrm{rel},\alpha}$ is the impact energy in channel $\alpha$, and $E_\alpha^0$ is the internal energy of the state or pseudostate $\alpha$. In the rest of this article we reset the overall zero of energy such that $E_1^0=0$ and $E=E_{\mathrm{rel},1}$.

In general, there will be a total of $N$ channels, $N_0$ of which are open. The $N$ coupled equations (4a) were solved numerically by a modified version of our Numerov code.[46] This code starts integrating at $r=r_0$, where $r_0$, is sufficiently small so that $f_{\alpha\alpha_0}(r_0)\cong0$ for all $\alpha$ and $\alpha_0$. We used $r_0=10^{-12}a_0$. In the asymptotic region, where the potential term of Eq. (4a) is negligible,

$$f_{\alpha\alpha_0}(r)=S_{\alpha\alpha}(r)A_{\alpha\alpha_0}+D_{\alpha\alpha}(r)B_{\alpha\alpha_0}\ , \tag{5}$$

where

$$S_{\alpha\alpha'}(r)=\begin{cases}\delta_{\alpha\alpha'}k_\alpha^{1/2}rj_{l_\alpha}(k_\alpha r), & k_\alpha^2>0\\ \delta_{\alpha\alpha'}\exp[\,|\,k_\alpha\,|\,(r-r_f)], & k_\alpha^2<0\end{cases} \tag{6}$$

$$D_{\alpha\alpha'}(r)=\begin{cases}-\delta_{\alpha\alpha'}\dfrac{k_\alpha^{1/2}}{2}rh_{l_\alpha}^{(1)}(k_\alpha r), & k_\alpha^2>0\\ \delta_{\alpha\alpha'}\{\exp[\,|\,k_\alpha\,|\,(r-r_f)]-i\exp[-\,|\,k_\alpha\,|\,(r-r_f)]\}, & k_\alpha^2<0\end{cases} \tag{7}$$

$j_l$ and $h_l^{(1)}$ are spherical Bessel functions of the first and third kind,[47] respectively, $r_f$ is a constant chosen to avoid overflow problems, and $A_{\alpha\alpha_0}$ and $B_{\alpha\alpha_0}$ are elements of the constant matrices $\underline{A}$ and $\underline{B}$. The generalized $N\times N$ $T$ matrix is then given by

$$\underline{T}=\underline{B}\,\underline{A}^{-1}\,, \tag{8}$$

and, if $N_0<N$, the transition matrix will be the upper left $N_0\times N_0$ submatrix of $\underline{T}$. It is clear that if $\underline{C}$ is any nonsingular $N\times N$ constant matrix, then the transformation

$$\underline{\tilde{f}}(r)=\underline{f}(r)\underline{C} \tag{9}$$

will give a new set of channel functions with

$$\tilde{f}_{\alpha\alpha_0}(r)=S_{\alpha\alpha}(r)\tilde{A}_{\alpha\alpha_0}+D_{\alpha\alpha}(r)\tilde{B}_{\alpha\alpha_0}\,, \tag{10}$$

and

$$\underline{T}=\underline{\tilde{B}}\,\underline{\tilde{A}}^{-1}\,. \tag{11}$$

When $N_0<N$, we use this fact to avoid linear dependence of the columns of $f$ by periodically making the transformation[48]

$$\underline{\tilde{f}}(r)=\underline{f}(r)[\underline{f}(r')]^{-1} \tag{12}$$

for all $r<r'$. Our program saves the $\underline{f}(r)$ at each integration point as well as the set of $r'$ values where any transformations were made. Once we know $\underline{T}$, this allows us to calculate a new solution matrix $\underline{F}(r)$ that is a continuous function of $r$ and satisfies

$$\underline{F}(r)\sim\underline{S}(r)+\underline{D}(r)\underline{T}\quad\text{as } r\to\infty\,. \tag{13}$$

It is useful to define an $r$-dependent $N\times N$ $\underline{T}$-matrix function by

$$\underline{T}(r)=2i\int_0^r dr'\,\underline{S}(r')\underline{V}^S(r')\underline{F}(r')\,. \tag{14}$$

By Green's theorem

$$\underline{T}=\underline{T}(\infty)\,. \tag{15}$$

For $n<N$, Wolken[41] showed how to find an $n\times n$ local optical-potential matrix with elements

$$V^{\rm opt}_{\alpha\alpha'}(r)=V^S_{\alpha\alpha'}(r)+Q^W_{\alpha\alpha'}(r),\quad \alpha,\alpha'=1,\ldots,n \tag{16}$$

that generates a new $n\times n$ solution matrix $\underline{G}(r)$ that reproduces the $n\times n$ upper-left subblock of $\underline{T}(r)$ for each value of $r$. By this we mean

$$\underline{T}_n(r)=2i\int_0^r dr'\,\underline{S}_n(r')[\underline{V}^S_n(r')+\underline{Q}^W(r')]\underline{G}(r')\,, \tag{17}$$

where $\underline{A}_n$ means the upper-left $n\times n$ subblock of the $N\times N$ matrix $\underline{A}$. As a consequence

$$\left[\frac{d^2}{dr^2}-\frac{l_\alpha(l_\alpha+1)}{r^2}+k_\alpha^2\right]G_{\alpha\alpha_0}(r)=\frac{2\mu}{\hbar^2}\sum_{\alpha'}[V^S_{\alpha\alpha'}(r)+Q^W_{\alpha\alpha'}(r)]G_{\alpha'\alpha_0}(r),\quad \alpha,\alpha'=1,\ldots,n \tag{18}$$

and

$$\underline{G}(r)\sim\underline{S}_n(r)+\underline{D}_n(r)\underline{T}_n\quad\text{as } r\to\infty\,. \tag{19}$$

We will call $\underline{Q}^W(r)$ the optical-correction potential. $\underline{Q}^W(r)$ is then given by

$$\underline{Q}^W(r)=[\underline{V}^S(r)\underline{F}(r)]_n[\underline{F}_n(r)]^{-1}-\underline{V}^S_n(r)\,. \tag{20}$$

$\underline{Q}^W(r)$ will be complex if $N_0$, the number of open channels in the original calculation, is greater than $n$; otherwise $\underline{Q}^W(r)$ will be real.

Although $\underline{V}^{\rm opt}(r)$ as defined by Eqs. (16) and (20) reproduces $\underline{T}_n(r)$ exactly, it has the undesirable property that it has a pole whenever the determinant of $\underline{F}_n(r)$ is zero. To obtain a more convenient effective potential we define a smoothed potential

$$\underline{V}^O(r)=\underline{V}^S_n(r)+\underline{Q}^O(r) \tag{21}$$

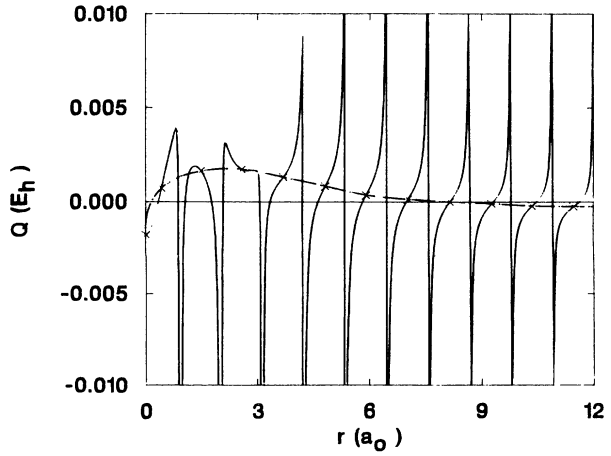


FIG. 1. Real part of the (1,1) element of the optical-correction potential (in $E_h$) as a function of $r$ (in $a_0$) for $n=1$, $E=4E_h$. In all figures, the symbols mark the $\{r_1\}$ used to generate $Q^O$. ——, $Q^W$; — — — and ×, $Q^O$.

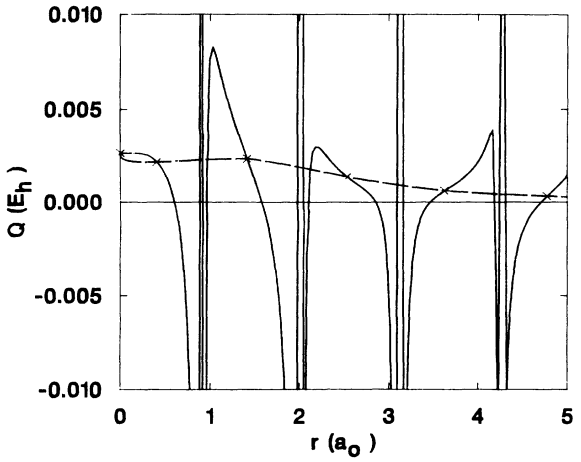


FIG. 2. Same as Fig. 1, except $n=2$.

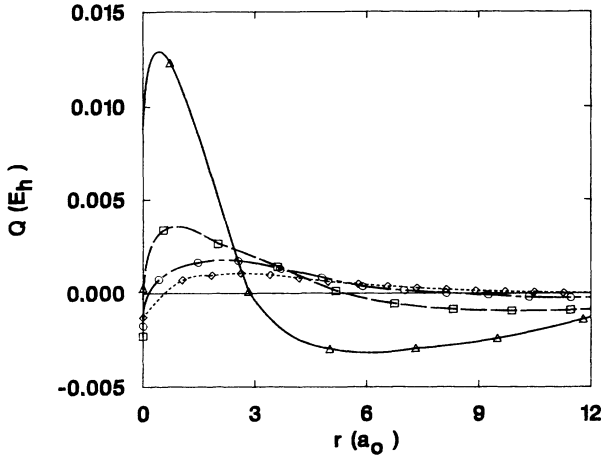


FIG. 3. Same as Fig. 1, except only $\mathrm{Re}\,Q^{O}_{11}$ for several energies. —— and △, $1.0E_h$; — — and □, $2.0E_h$; —· and ○, $4.0E_h$; - - - and ◇, $8.0E_h$.

in terms of a smoothed optical-correction potential $\underline{Q}^{O}(r)$ such that $\underline{Q}^{O}(r_i)=\underline{Q}^{W}(r_i)$ for $r_i$ an element of the set $\{r_i\}$, where $\{r_i\}$ contains points where $\underline{Q}^{W}(r)$ has no poles. For the case $n=1$, the set $\{r_i\}$ was chosen to contain the values of $r$ where $|F_{11}(r)|$ has a local maximum, and $r_0$, the starting point of the integration of Eq. (4a). This means we have a point about halfway between each singularity. Figure 1 shows $\mathrm{Re}Q^{W}_{11}(r)$ and $\mathrm{Re}Q^{O}_{11}(r)$ for the example problem of Sec. II with $N=5$, $n=1$, and at $E=4E_h$. The behavior of the imaginary parts is quite similar.

For $n=2$, we used an extension of the above rule. The extension is motivated by the fact that, for the example problem of Sec. II, the singularities of $\underline{Q}^{W}(r)$ occur in pairs; see Fig. 2. This happens because the local maxima of $|\det\underline{F}_n(r)|$ occur in pairs, with one of the two in the pair much bigger than the other. The extended rule is as follows. If the local maxima of $|\det\underline{F}_n(r)|$ occur at $r$ equal to $d_1,d_2,\ldots,$ and if $D_i=|\det\underline{F}_n(d_i)|$, we compare $D_i$ to $D_{i+1}$, and if $D_i\le\epsilon D_{i+1}$, $d_i$ is not included in the set $\{r_i\}$. In addition, $r_0$ is included in $\{r_i\}$. For the case considered in this paper, $\epsilon=0.5$ and 0.9 gave the same results for $r<14a_0$, and in this $r$ range these choices correspond to including one $r_i$ between every other singularity. This is shown in Fig. 2 for the real part of $Q^{W}_{11}$ for $N=5$, $n=2$, $E=4E_h$, and $\epsilon=0.9$. This rule, when applied with any $\epsilon\le 0.9$ to any of the $n=1$ cases considered in this article, generates precisely the same $\{r_i\}$ as the original rule at all $r$. For either $n=1$ or $n=2$, to generate $\underline{Q}^{O}(r)$ for all $r$, four-point or six-point Lagrangian interpolation was used with the values at the selected $\{r_i\}$ as the input set.

In the discussion to follow it will be interesting to compare the real part of $Q^{O}_{11}(r)$ to the adiabatic polarization potential $V^{Pa}(r)$. This is obtained as follows.[27,49] If $H^{e}(r)$ is the Hamiltonian for a hydrogen atom in the presence of an electron fixed a distance $r$ from the nucleus, then $V^{Pa}(r)$ is defined as

$$V^{Pa}(r)=E^{e}_1(r)-E^{0}_1-V^{S}_{11}(r)\,, \tag{22}$$

where $E^{e}_1(r)$ is the lowest eigenvalue found by diagonalizing $H^{e}(r)$ in the five-state basis used here, $V^{S}_{11}(r)$ is the static potential which is defined in Eq. (4d), and

$$E^{0}_1=E^{e}_1(r=\infty)\,. \tag{23}$$

TABLE II. Phase shifts (rad) in the 1$s$ channel for $n=1$.

| $E$ ($E_h$) | $N_0$ | Exact[a] | Optical-correction potential Smoothed[b] | Smoothed[c] | Adiabatic[d] | None[e] |
|---|---|---|---|---|---|---|
| 0.2 | 1 | 1.780 | 1.745 | 1.867 | 1.776 | 1.012 |
| 0.4 | 2 | 0.6711+$i$0.0975 | 0.6710+$i$0.0974 | 0.6796+$i$0.0967 | 1.435 | 0.9356 |
| 1.0 | 5 | 0.8080+$i$0.1177 | 0.8034+$i$0.1118 | 0.8060+$i$0.1150 | 1.137 | 0.8028 |
| 2.0 | 5 | 0.6939+$i$0.0599 | 0.6939+$i$0.0589 | | 0.9401 | 0.6949 |
| 4.0 | 5 | 0.5883+$i$0.0299 | 0.5886+$i$0.0297 | | 0.7691 | 0.5899 |
| 8.0 | 5 | 0.4909+$i$0.0148 | 0.4911+$i$0.0145 | | 0.6224 | 0.4919 |

[a]From Eq. (18) with $n=1$, $N=5$. This agrees to at least the number of significant figures given with what is obtained from the full five-state calculation.
[b]Based on four-point Lagrangian interpolation of $Q^{O}_{11}(r_i)$.
[c]Based on six-point Lagrangian interpolation of $Q^{O}_{11}(r_i)$. This is given only when it differs significantly from the results using four-point interpolation.
[d]Obtained using $V^{\mathrm{opt}}_{11}(r)=V^{S}_{11}(r)+V^{Pa}(r)$.
[e]Obtained using $V^{\mathrm{opt}}_{11}(r)=V^{S}_{11}(r)$.

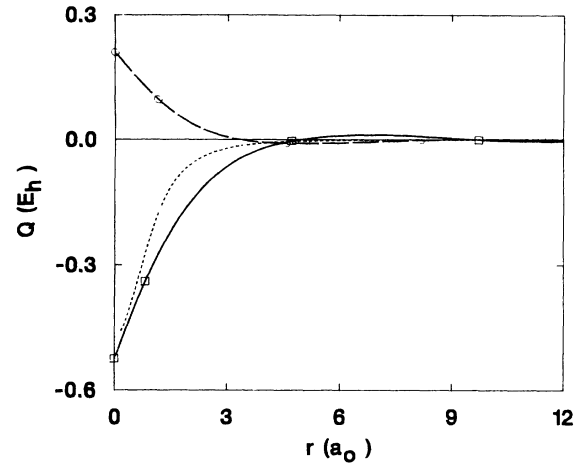


FIG. 4. Same as Fig. 3, except $V^{Pa}$ is also shown. —— and □, $0.2E_h$; — — and ○, $0.4E_h$; and - - -, $V^{Pa}$.

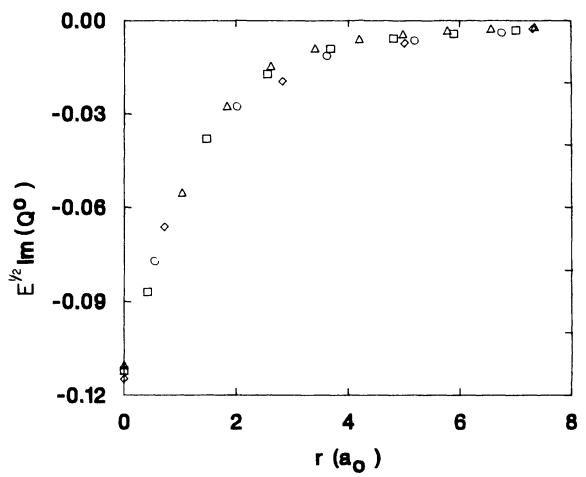


FIG. 6. $\sqrt{E} \times \mathrm{Im}Q^o_{11}$ (in $E_h^{3/2}$) for $n=1$ as a function of $r$ (in $a_0$) for several energies $E$. The kind of symbol denotes the energy: ◇, $1E_h$; ○, $2E_h$; □, $4E_h$; △, $8E_h$.

## IV. RESULTS AND DISCUSSION

We now consider applying the methods of Sec. III to the example of Sec. II. In all cases we use $N=5$.

Table II shows the phase shifts obtained by solving Eq. (18) for $n=1$ for three different optical-correction potentials along with the results using no optical-correction potential. For $E \geq 2E_h$, the smoothed optical potential reproduces the phase shifts of the full five-state calculation within $0.0003-i0.0010$. At $0.4-1.0E_h$, the differences are less than or equal to $0.008+i0.008$. At the lowest energy $0.2E_h$ the agreement is still excellent, with a discrepancy of only 0.03 or 0.09, depending on the order of interpolation. The larger discrepancies at lower energies are due to the smaller number of points used in the smoothing procedure and the problem of interpolating between them. [Our algorithm involves fewer points at lower energies because there are fewer poles of $\underline{Q}^W(r)$ there.]

In contrast to $Q^o_{11}(r)$, the adiabatic polarization potential does quite poorly, except for the lowest energy where $N_0=n$. In fact, for the five highest energies considered here, it would be better to use no optical-correction potentials at all, rather than to use the adiabatic polarization potential.

Figures 3–8 show various aspects of the optical-correction potentials used for the calculations in Table II. Figures 3 and 4 show the short-range real part of $Q^o_{11}(r)$ at the energies studied along with the adiabatic polarization potential. For the four highest energies, shown in Fig. 3, $\mathrm{Re}Q^o_{11}(r)$ is quite small and is positive near the origin, but it goes to zero, or slightly negative, at the origin. In the important small-$r$ region, as the energy is increased, $\mathrm{Re}Q^o_{11}(r)$ gets smaller and the position of the positive maximum moves to larger $r$. As an interesting consequence, $\mathrm{Re}Q^o_{11}(r)$ is positive over most of the range illustrated in Fig. 3. The quantitative results, of course, de-

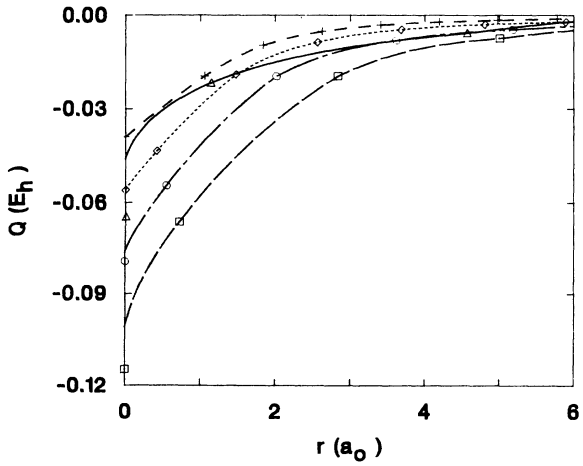


FIG. 5. Same as Fig. 3, except only $\mathrm{Im}Q^o_{11}$ for several energies. —— and △, $0.4E_h$; — — and □, $1.0E_h$; —- and ○, $2.0E_h$; - - - and ◇, $4.0E_h$; and — — — and ×, $8.0E_h$.

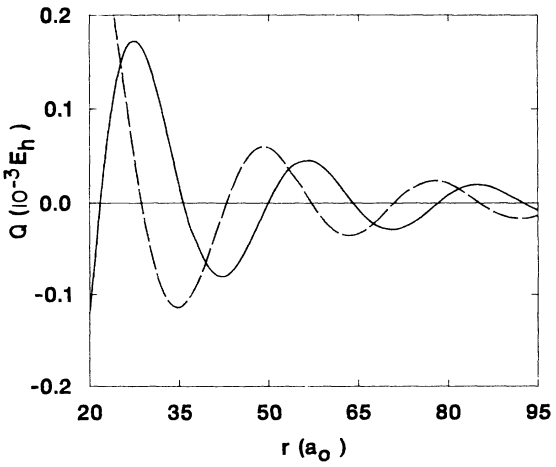


FIG. 7. $\mathrm{Re}Q^o_{11}$ and $\mathrm{Im}Q^o_{11}$ (in $10^{-3}E_h$) as functions of $r$ (in bohrs) for $n=1$, $E=2E_h$. In this $r$ region, the $\{r_i\}$ occur at about every $0.8a_0$. ——, Re; — —, Im.

TABLE III. Parameters for the fits $[V^{Pa}(r)$ or $Q_{11}^{O}(r)]=-(a/2r^{\not\alpha})\exp[i(\not\alpha r+c)]$, for $m=1$.

| $E$ ($E_h$) | $a$ ($E_h a_0^{\not\alpha}$) | $\not\alpha$ | $\not\alpha$ ($a_0^{-1}$) | $c$ |
|---|---|---|---|---|
| adiabatic | 4.57[a] | 4.00 | 0.0 | 0.0 |
| 0.2 | 4.40 | 3.99 | 0.0 | 0.0 |
| 0.4 | 35.4 | 3.97 | −0.664 | 4.417 |
| 1.0 | 0.496 | 2.02 | −0.337 | 3.372 |
| 2.0 | 0.226 | 1.94 | −0.223 | 3.260 |
| 4.0 | 0.140 | 1.94 | −0.152 | 3.135 |
| 8.0 | 0.103 | 2.00 | −0.105 | 3.048 |

[a] $a$ is not equal to $4.50E_h a_0^{\not\alpha}$ here because the quadrupole polarizability contributes a $r^{-6}$ term, and, for consistency, this row is based on a least-squares fit over the range (20−80) $a_0$ using the same set of $r_i$ as for the next row.

pend on the procedure we have used to smooth $\underline{Q}^{W}(r)$. Thus, it is significant that the shape of $\mathrm{Re}Q_{11}^{O}(r)$ does not change radically as a function of energy; this lends further support to the reasonableness of the smoothing method. For the lower energies, Fig. 4 shows $\mathrm{Re}Q_{11}^{O}$ along with the adiabatic polarization potential. Here, the shape is different. At $0.4E_h$, $\mathrm{Re}Q_{11}^{O}$ has a positive peak at the origin, but both $\mathrm{Re}Q_{11}^{O}$ at $0.2E_h$ and $V^{Pa}$ have negative peaks there. Note also that $\mathrm{Re}Q_{11}^{O}$ is much larger in Fig. 4 than in Fig. 3. In comparison to $V^{Pa}$, $\mathrm{Re}Q_{11}^{O}$ for $0.2E_h$ has two points near the origin more negative than $V^{Pa}$. This is unexpected since physically $V^{Pa}$ would be expected to be a bound to the true polarization potential. The bound is not rigorous, though, since the optical potential is not negative everywhere. Note also that only the first two points of $\mathrm{Re}Q_{11}^{O}$ at $0.2E_h$ are more negative than $V^{Pa}$; all others lie above $V^{Pa}$, and it is possible that an alternative smoothing procedure would reverse the trend at the first two points.

Figure 5 shows the imaginary part of $Q_{11}^{O}$ for all of the energies used. $\mathrm{Im}Q_{11}^{O}$ always has a negative peak at the origin and is larger at small $r$ than $\mathrm{Re}Q_{11}^{O}$, except for the lowest energy. In addition, if the lowest energy is excluded, $\mathrm{Im}Q_{11}^{O}$ changes very smoothly with energy. In fact, Fig. 6, which combines the points for the range $1-8E_h$, shows that $\sqrt{E}\times\mathrm{Im}Q_{11}^{O}$ is almost independent of energy. At the lowest energy, $\mathrm{Im}Q_{11}^{O}$ has a slightly different shape

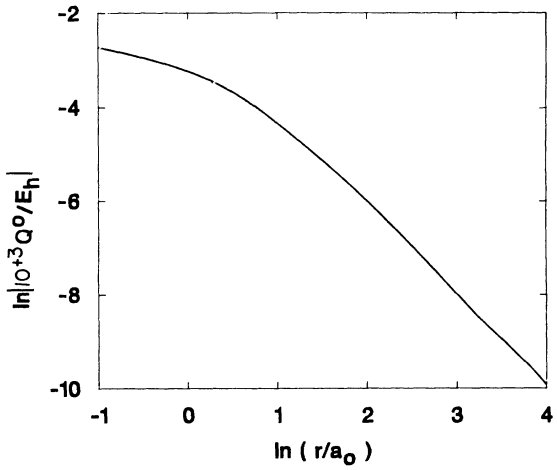


FIG. 8. $\ln|Q_{11}^{O}|$ (with $Q_{11}^{O}$ in $10^{-3}E_h$) as a function of $\ln r$ (with $r$ in bohrs) for $n=1$, $E=2E_h$.

and is smaller than would be predicted from the other energies. This is because $\mathrm{Im}Q_{11}^{O}$ must go to zero at the $2s$ threshold of $0.375E_h$.

Figures 7 and 8 show the long-range part of $Q_{11}^{O}$ for an energy of $2E_h$. In Fig. 7 we see that $Q_{11}^{O}$ oscillates with the real and imaginary parts out of phase by about $\pi/2$. Figure 8 shows that $\ln|Q_{11}^{O}|$ is a very smooth function of $r$ without oscillations. This is typical behavior for all of the energies studied here above the $2s$ threshold. In fact, the long-range part of $Q_{11}^{O}$ can be fitted quite well by

$$Q_{11}^{O}(r)=-(a/2r^{\not\alpha})\exp[i(\not\alpha r+c)]\ . \tag{24}$$

Values of the parameters $a$, $\not\alpha$, $c$, and $\not\alpha$ for each energy studied here are given in Table III. These are the best values in the least-squares sense which fit $Q_{11}^{O}(r_i)$ for $20<r_i<80a_0$. For energies greater than $1E_h$, $\not\alpha$ is very close to 2, while for lower energies, $\not\alpha$ is close to 4. The coefficient $a$ decreases with increasing energy for energies greater than $0.4E_h$, and for the lowest energy where $n=N_0$, $a$ is slightly lower than the value for the adiabatic polarization potential. The factors $\not\alpha$ and $c$ are zero for the lowest energy since the optical-correction potential is real. For higher energy, the magnitudes of $\not\alpha$ and $c$ de-

TABLE IV. $T$-matrix elements for $n=2$.

| $E$ ($E_h$) | Transition | Exact[a] | Optical-correction potential Smoothed[b] | Smoothed[c] | None[d] |
|---|---|---|---|---|---|
| 4.0 | 1s-1s | −0.638+i0.870 | −0.639+i0.869 | | −0.623+i0.908 |
| | 1s-2s | 0.170+i0.009 | 0.168+i0.009 | | 0.181+i0.022 |
| | 2s-2s | −1.545+i0.725 | −1.553+i0.722 | | −1.581+i0.793 |
| 0.4 | 1s-1s | −0.814+i0.801 | −1.036+i0.811 | −0.881+i0.817 | −1.216+i0.822 |
| | 1s-2s | −0.568+i0.027 | −0.600+i0.066 | −0.581+i0.054 | −0.484+i0.211 |
| | 2s-2s | −1.109+i0.816 | −1.142+i0.799 | −1.268+i0.782 | −0.251+i0.401 |

[a] From Eq. (18) with $n=2$, $N=5$. This agrees to at least the number of significant figures given with what is obtained from the full five-state calculation.
[b] Based on four-point Lagrangian interpolation of $\underline{Q}^{O}(r_i)$.
[c] Based on six-point Lagrangian interpolation of $\underline{Q}^{O}(r_i)$. This is given only when it differs significantly from the results using four-point interpolation.
[d] Based on two-channel calculation with $V_{\alpha\alpha'}^{\mathrm{opt}}=V_{\alpha\alpha'}^{S}$.

crease with increasing energy, with $b$ always negative. In the high-energy limit, it appears that $a$ and $b$ go smoothly to zero, while $p$ will remain close to 2. The phase correction $c$ is only determinable within an additive multiple of $2\pi$ so it is uncertain what its limit is or if it has a limit.

As mentioned above, at sufficiently large $r$, $\mathrm{Re}Q^O_{11}(r)$ for $E$ equal to $0.2E_h$ may be fitted by $-a/2r^4$ with $a$ close to the value obtained from the large-$r$ limit of the adiabatic polarization potential. This is significant because for collision energies below the first electronic threshold it can be rigorously established that[16,50–52]

$$V^P(r) \sim -e^2\alpha_{1s\,1s}/2r^4 \text{ as } r\to\infty \ , \tag{25}$$

where $\alpha_{1s\,1s}$ is the static electric dipole polarizability [which is a special case of Eq. (27) below]. Our agreement with this form is an encouraging success for the present method of localizing the optical potential. Since our smoothing procedure yields the correct large-$r$ limit below the first electronic threshold, we have more confidence that it may be useful in studying the energy dependence of the absorption and polarization potentials at higher energies.

Table IV shows the $2\times2$ transition matrices found using $\underline{Q}^W$ and $\underline{Q}^O$, along with no optical potential, for cases with $n=2$, $N=5$ at two energies. These transition matrices for the $\underline{Q}^O$ calculations were found by matching to the $T$ matrix boundary conditions of Eq. (5) and symmetrizing the $T$ matrix by taking the arithmetic average of the off-diagonal elements. At $E=4E_h$, the symmetrized $T$-matrix elements differ from the unsymmetrized ones by 3% or less.

The agreement between the $\underline{Q}^O$ calculation and the $\underline{Q}^W$ calculation is quite good at the highest energy, but not as good for the lowest energy where $\underline{Q}^O$ is real. This is due to the problem of interpolating between only a few points. In spite of this, at the lowest energy using $\underline{Q}^O$ is an improvement over using no optical-correction potential at all.

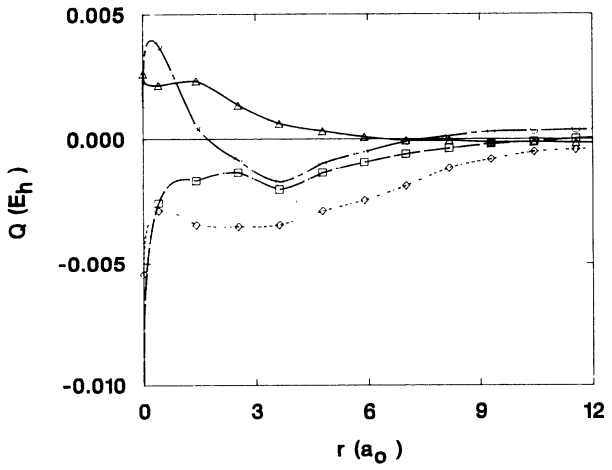


FIG. 9. Real parts of the smoothed optical-correction-potential matrix elements (in $E_h$), labeled by $\alpha,\alpha'$, as functions of $r$ (in $a_0$) for $n=2$, $E=4E_h$. —— and △, $1s\,1s$; —— and □, $1s\,2s$; —- and ○, $2s\,1s$; - - - and ◇, $2s\,2s$.

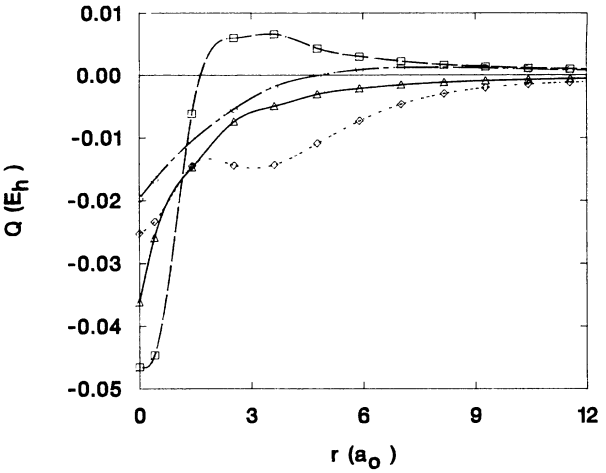


FIG. 10. Same as Fig. 9, except now the imaginary part.

Figures 9–11 show the short-range part of the $\underline{Q}^O$ matrices used for Table IV. Figure 9 shows the real part of $\underline{Q}^O$ at an energy of $4E_h$, Fig. 10 shows the imaginary part of $\underline{Q}^O$ at $4E_h$, and Fig. 11 shows $\underline{Q}^O$ at $0.4E_h$. As required to cause flux loss, $\underline{Q}^O$ is non-Hermitian in both cases. The figures show that the $2\times2$ optical-potential elements have a more complicated $r$ dependence than for $n=1$. $\mathrm{Re}\underline{Q}^O$ is much smaller at $4E_h$ than it is at $0.4E_h$. The long-range behavior of $\underline{Q}^O$ is quite complicated. Examination of a larger $r$ range than shown in the figures indicates that the components of $\underline{Q}^O$ at $4E_h$ come in pairs which oscillate out of phase by $\pi/2$. The pairs are $(\mathrm{Re}Q^O_{11},\mathrm{Re}Q^O_{21})$, $(\mathrm{Im}Q^O_{11},\mathrm{Im}Q^O_{21})$, $(\mathrm{Re}Q^O_{12},\mathrm{Re}Q^O_{22})$, and $(\mathrm{Im}Q^O_{12},\mathrm{Im}Q^O_{22})$.

It is interesting to compare the optical-correction-potential matrix elements for $n=2$ to the adiabatic asymptotic limit of the matrix polarization potential representing the effect of states not included in the $n=2$ pair. This is given by the electric dipole approximation and second-order perturbation theory. For the present case where the $n=2$ pair consists of $s$ states, this yields

$$V^P_{\alpha\alpha'}(r) \sim -e^2\alpha_{\alpha\alpha'}/(2r^4) \text{ as } r\to\infty \ , \tag{26}$$

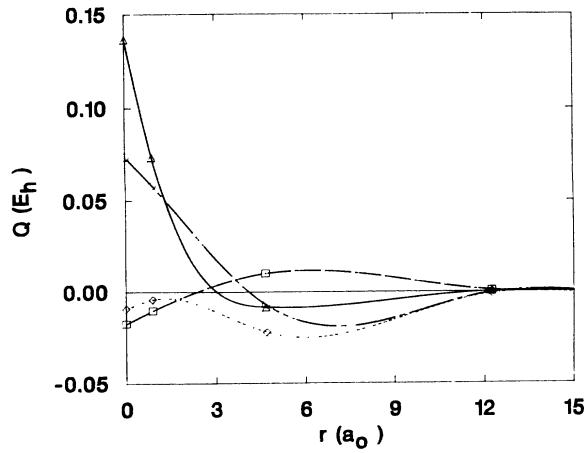


FIG. 11. Same as Fig. 9, except $E=0.4E_h$ at $r=0-15a_0$.

TABLE V. Static electric dipole transition polarizabilities (in $a_0^3$).

| $\alpha$ | $\alpha'$ | $\alpha_{\alpha\alpha'}$ |
|---|---|---|
| 1s | 1s | 4.5 |
| 1s | 2s | −6.9527 |
| 2s | 1s | −66.746 |
| 2s | 2s | 103.126 |

where

$$\alpha_{\alpha\alpha'}=\tfrac{2}{3}\sum_{\beta}\frac{\mu_{\alpha\beta}\mu_{\beta\alpha'}}{E_\beta^0-E_\alpha^0}\ . \tag{27}$$

$\alpha_{\alpha\alpha'}$ is the static electric dipole transition polarizability, the sum is over the radial parts of all $p$ states connected to the initial and final state by a dipole transition, and

$$\mu_{\alpha\beta}=e\int_0^\infty R_\alpha(r)rR_\beta(r)r^2dr\ , \tag{28}$$

where $R_\alpha(r)$ is the radial part of the target wave function in state $\alpha$. For the basis of Sec. II, the sum in Eq. (27) consists of only one term involving the $\overline{2p}$ state. Table V gives the results.

Figures 12 and 13 show the long-range behavior of $\underline{\underline{Q}}^O$ at $0.4E_h$ along with the adiabatic asymptotic limit. Figure 12 shows that $Q_{11}^O$ and $Q_{21}^O$ oscillate out of phase by about $\pi$ with the maxima about 2 to 3 times greater than the values calculated from Eq. (26) and Table V. In Fig. 13 we see that $Q_{12}^O$ is always positive and $Q_{22}^O$ always negative, and both lie very close to what is predicted by Eq. (26). $Q_{12}^O$ and $Q_{22}^O$, however, do show periodic deviations from this form; at these points $Q_{12}^O$ and $Q_{22}^O$ are less in magnitude than predicted by Eq. (26). Figure 11 shows that the sign of $Q_{22}$ persists at all $r$ and the sign of $Q_{12}$,

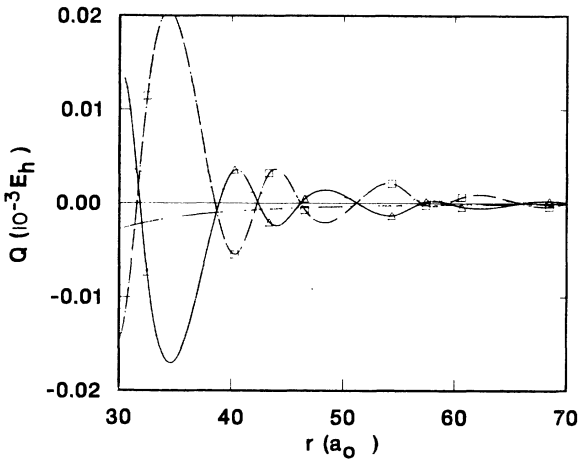


FIG. 12. Real parts of the smoothed optical-correction-potential matrix elements $Q_{11}^0$ and $Q_{21}^0$ (in $10^{-3}E_h$) for $n=2$, $E=0.4E_h$, as compared to asymptotic forms of adiabatic polarization potentials. For the smoothed optical-correction potentials, the curves are the smoothed results, and the symbols are for the $\{r_i\}$ used as input to the smoothing algorithm. — — — and □, $Q_{21}^0$; - - -, $-\alpha_{21}/(2r^4)$; —-, $-\alpha_{11}/(2r^4)$; —— and △, $Q_{11}^0$.

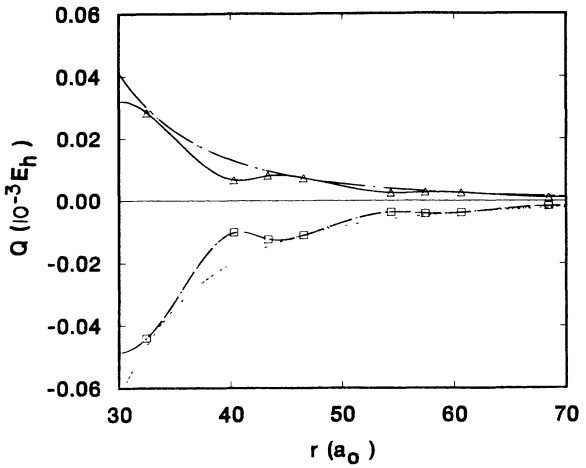


FIG. 13. Same as Fig. 12, except: —-, $-\alpha_{12}/(2r^4)$; —— and Δ, $Q_{12}^0$; — — — and □, $Q_{22}^0$; - - -, $-\alpha_{22}/(2r^4)$.

which is explained at large $r$ by Fig. 13, persists to $r\simeq 3a_0$. We conclude that Eq. (26), although it clearly does not explain the detailed structure, does explain some of the general features of the optical-correction potentials, including the opposite signs of $Q_{12}^0$ and $Q_{22}^0$ at large $r$.

## V. CONCLUSIONS

We have developed a simple smoothing procedure for optical potentials such that the smoothed optical potentials still reasonably accurately reproduce a submatrix of the full scattering matrix of a larger calculation. The real and imaginary parts of the resulting smoothed optical-correction potentials may be considered as dynamically accurate, nonempirical versions of the polarization and absorption terms of the effective-potential approach to electron scattering.

The most striking aspect of the present results is that the accurate polarization potentials look very different from those for the usual methods; they show a strong energy dependence, and except at very low energy they are positive in most of the region within $3a_0$ of the nucleus. At 50 eV and above they are even positive in the $3-5a_0$ intermediate-$r$ region. It would be very interesting to test the effect of introducing this kind of behavior into the model potentials that are widely used for applications.

The adiabatic asymptotic limit of the polarization potential is given by Eq. (26), and it is well known to be a rigorous result only below the first electronic excitation threshold.[16,50–52] Our results confirm this form at low energy, but at high energy they yield an oscillatory polarization potential whose envelope scales with energy and distance as $E^{-1/2}r^{-2}$.

There is very little known about the $r$ and $E$ dependence required for an accurate absorption potential. Available models differ even for the question of whether such a potential should peak at the nucleus or not. The absorption potential yielded by the eikonal optical model[22] peaks at the nucleus, but the empirical absorption potentials of McCarthy and Green and coworkers[36,37] and the

dispersion-relation absorption potential[38] based on the energy-dependent polarization potential of Onda and one of the authors[28] peak at nonzero $r$. The absorption potential yielded by the quasifree scattering model peaks away from the nucleus at the energies considered in the present paper, but the peak moves to the nucleus at very high energy.[32] In contrast, Figs. 5, 6, and 10 show that the accurate dynamical absorption potential of the present work peaks at the nucleus. In Green's empirical absorption potential the peak position is independent of energy, but in the other cases where the absorption potential peaks away from the nucleus, the peak position moves in as the energy increases. Figures 5 and 6 show that, except near threshold, the present absorption potential becomes weaker at all $r$ as the energy is increased and retains its shape as a function of $r$. This qualitative characteristic is in good agreement with the phenomenological approach of Green *et al.*[37] who assume that $V^A(r)$ factors into a function of $E$ times a function of $r$. Their limiting $E$ dependence is $E^{-1}\ln E$, which is steeper than the $E^{-1/2}$ found here.

Although the concepts of elastic optical potential, polarization potential, and absorption potential are widely used, there has been much less work on off-diagonal (inelastic) elements of the generalized-optical potential. Local approximations to the off-diagonal elements have, however, been studied by Feshbach theory, perturbation theory, and models.[51,53–57] The adiabatic asymptotic limit is given by Eq. (26). We find that even for an energy at which the $\overline{2p}$ state is closed, the adiabatic asymptotic limit provides a poor representation of the exact dynamical optical-correction potential. This indicates that an expansion approach in which the first term is the adiabatic approximation and higher terms are nonadiabatic corrections is more slowly convergent for the inelastic optical-correction potential than for the elastic one. This agrees with the conclusion of Mittleman,[51] based on a more qualitative analysis, and with the conclusion of Rice *et al.*,[55] based on a semiempirical analysis of experimental data. It is our hope that the techniques of smoothed optical-correction potentials will provide useful guidance for the development of physically correct polarization and absorption potentials in future work.

## ACKNOWLEDGMENTS

The authors are grateful to Joseph Abdallah, Jr. for his help in the early stages of this research. This work was supported in part by the National Science Foundation through Grant No. CHE-80-25232.

[1]K. Smith, *The Calculation of Atomic Collision Processes* (Wiley-Interscience, New York, 1971).
[2]P. G. Burke and W. D. Robb, Adv. At. Mol. Phys. 11, 143 (1975).
[3]R. K. Nesbet, Adv. Quantum Chem. 9, 215 (1975); Adv. At. Mol. Phys. 13, 315 (1977).
[4]J. Callaway, Phys. Rep. 45, 89 (1978).
[5]H. Feshbach, Ann. Phys. (N.Y.) 5, 357 (1958); 19, 287 (1962).
[6]J. S. Bell and E. J. Squires, Phys. Rev. Lett. 3, 96 (1959).
[7]A. L. Fetter and K. M. Watson, Adv. Theor. Phys. 1, 115 (1965).
[8]R. T. Pu and E. S. Chang, Phys. Rev. 151, 31 (1966).
[9]H. P. Kelly, Phys. Rev. 160, 44 (1967); 166, 47 (1968); 171, 54 (1968); Adv. Chem. Phys. 14, 129 (1969).
[10]G. D. Alton, W. R. Garrett, M. Reeves, and J. E. Turner, Phys. Rev. A 6, 2138 (1972); P. W. Coulter and W. R. Garrett, *ibid.* 18, 1902 (1978); 23, 2213 (1981).
[11]M. Knowles and M. R. C. McDowell, J. Phys. B 6, 300 (1973).
[12]G. Csanak, H. S. Taylor, and R. Yaris, Adv. At. Mol. Phys. 7, 287 (1971); B. Yarlagadda, G. Csanak, H. S. Taylor, B. Schneider, and R. Yaris, Phys. Rev. A 7, 146 (1973); L. D. Thomas, G. Csanak, H. S. Taylor, and B. S. Yarlagadda, J. Phys. B 7, 1719 (1974); T. Scott and H. S. Taylor, *ibid.* 12, 3367 (1979); 12, 3385 (1979).
[13]K. H. Winters, C. D. Clark, B. H. Bransden, and J. P. Coleman, J. Phys. B 7, 788 (1974); T. Scott and B. H. Bransden, *ibid.* 14, 2277 (1981); B. H. Bransden, T. Scott, R. Shingal, and R. K. Roychoudhury, *ibid.* 15, 4605 (1982).
[14]A. Klonover and U. Kaldor, J. Phys. B 11, 1623 (1978).
[15]I. E. McCarthy, B. C. Saha, and A. T. Stelbovics, J. Phys. B 15, L401 (1982); I. E. McCarthy and A. T. Stelbovics, *ibid.* 16, 1233 (1983).
[16]M. H. Mittleman and K. M. Watson, Phys. Rev. 113, 198 (1959).
[17]B. L. Moiseiwitsch, Proc. Natl. Acad. Sci. India 33, 537 (1963).
[18]J. Callaway, R. W. LaBahn, R. T. Pu, and W. M. Duxler, Phys. Rev. 168, 12 (1968); W. M. Duxler, R. T. Poe, and R. W. LaBahn, Phys. Rev. A 4, 1935 (1971).
[19]C. J. Joachain and M. H. Mittleman, Phys. Rev. A 4, 1492 (1971).
[20]R. J. Drachman and A. Temkin, Case Stu. At. Coll. Phys. 2, 399 (1972).
[21]G. Csanak and H. S. Taylor, Phys. Rev. A 6, 1843 (1972).
[22]F. W. Byron, Jr. and C. J. Joachain, Phys. Rev. A 9, 2559 (1974); 15, 128 (1977); Phys. Rep. 34C, 233 (1977); C. J. Joachain, R. Vanderpoorten, K. H. Winters, and F. W. Byron, Jr., J. Phys. B 10, 227 (1977).
[23]B. L. Jhanwar and S. P. Khare, Phys. Lett. 50A, 201 (1974); J. Phys. B 9, L527 (1976); B. L. Jhanwar, S. P. Khare, and A. Kumar, Jr., *ibid.* 11, 887 (1978).
[24]R. Vanderpoorten, J. Phys. B 8, 926 (1975).
[25]H. R. J. Walters, J. Phys. B 9, 227 (1976).
[26]S. Hayashi and K. Kuchitsu, Chem. Phys. Lett. 44, 1 (1976); J. Phys. Soc. Jpn. 42, 621 (1977).
[27]D. G. Truhlar and F. A. Van-Catledge, J. Chem. Phys. 69, 3575 (1978); K. Onda and D. G. Truhlar, *ibid.* 70, 1681 (1979); D. G. Truhlar, D. A. Dixon, R. A. Eades, F. A. Van-Catledge, and K. Onda in *Electron-Molecule and Photon-Molecule Collisions,* edited by T. N. Rescigno, V. McKoy, and B. I. Schneider (Plenum, New York, 1979), p. 151; D. G. Truhlar, K. Onda, R. A. Eades, and D. A. Dixon, Int. J. Quantum Chem. Symp. 13, 601 (1979).
[28]K. Onda and D. G. Truhlar, Phys. Rev. A 22, 86 (1980).
[29]D. G. Truhlar in *Chemical Applications of Atomic and Molecular Electrostatic Potentials,* edited by P. Politzer and D. G. Truhlar (Plenum, New York, 1981), p. 123.
[30]S. M. Valone, D. G. Truhlar, and D. Thirumalai, Phys. Rev.

A 25, 3003 (1982); D. Thirumalai and D. G. Truhlar, *ibid.* 27, 158 (1983); N. Abusalbi, R. A. Eades, T. Nam, D. Thirumalai, D. A. Dixon, D. G. Truhlar, and M. Dupuis, J. Chem. Phys. 78, 1213 (1983).

[31]J. K. O'Connell and N. F. Lane, Phys. Rev. A 27, 1893 (1983).

[32]G. Staszewska, D. W. Schwenke, D. Thirumalai, and D. G. Truhlar, J. Phys. B 16, L281 (1983); Phys. Rev. A 28, 2740, (1983); G. Staszewska, D. W. Schwenke, and D. G. Truhlar, Int. J. Quantum Chem. Symp. (in press).

[33]P. G. Burke and N. Chandra, J. Phys. B 5, 1696 (1972).

[34]M. A. Morrison, N. F. Lane, and L. A. Collins, Phys. Rev. A 15, 2186 (1977); J. R. Rumble, Jr., D. G. Truhlar, and M. A. Morrison, J. Phys. B 14, L301 (1981).

[35]F. A. Gianturco and D. G. Thompson in *Electron-Atom and Electron-Molecule Collisions,* edited by J. Hinze (Plenum, New York, 1983), p. 231.

[36]J. B. Furness and I. E. McCarthy, J. Phys. B 7, 541 (1974); I. E. McCarthy, C. J. Noble, B. A. Phillips, and A. D. Turnbull, Phys. Rev. A 15, 2173 (1977).

[37]A. E. S. Green, D. E. Rio, and T. Ueda, Phys. Rev. A 24, 3010 (1981).

[38]S. M. Valone, D. Thirumalai, and D. G. Truhlar, Int. J. Quantum Chem. Symp. 15, 341 (1981); D. Thirumalai and D. G. Truhlar, Phys. Rev. A 26, 793 (1982).

[39]G. Staszewska, D. W. Schwenke, and D. G. Truhlar, Phys. Rev. A 28, 169 (1983).

[40]D. Thirumalai, D. G. Truhlar, M. A. Brandt, R. A. Eades, and D. A. Dixon, Phys. Rev. A 25, 2946 (1982); D. Thirumalai and D. G. Truhlar, *ibid.* 25, 3058 (1982).

[41]G. Wolken, Jr., J. Chem. Phys. 56, 2591 (1972).

[42]A. Temkin, Phys. Rev. 116, 358 (1959).

[43]R. Damburg and E. Karule, Proc. Phys. Soc. 90, 637 (1967).

[44]P. G. Burke and J. F. B. Mitchell, J. Phys. B 6, 320 (1973).

[45]A. R. Edmonds, *Angular Momentum in Quantum Mechanics* (Princeton University, Princeton, 1957).

[46]D. G. Truhlar, N. M. Harvey, K. Onda, and M. A. Brandt, in *Algorithms and Computer Codes for Atomic and Molecular Quantum Scattering Theory,* edited by L. Thomas (National Resource for Computation in Chemistry, Lawrence Berkeley Laboratory, Berkeley, CA, 1979), Vol. I, p. 222.

[47]*Handbook of Mathematical Functions,* U. S. Natl. Bur. Stand. (Appl. Math. Ser. No. 55), edited by M. Abramowitz and I. A. Stegun (U.S. GPO, Washington, D.C., 1964).

[48]M. E. Riley and A. Kuppermann, Chem. Phys. Lett. 1, 537 (1968).

[49]D. G. Truhlar, D. A. Dixon, and R. A. Eades, J. Phys. B 12, 1913 (1979); R. A. Eades, D. A. Dixon, and D. G. Truhlar, J. Phys. B 15, 3365 (1982).

[50]L. Castillejo, I. C. Percival, and M. J. Seaton, Proc. Soc. London, Ser. A 254, 259 (1960).

[51]M. H. Mittleman, Ann. Phys. (N.Y.) 14, 94 (1961).

[52]C. J. Kleinman, Y. Hahn, and L. Spruch, Phys. Rev. 165, 53 (1968).

[53]M. H. Mittleman and R. Pu, Phys. Rev. 126, 370 (1962); M. H. Mittleman, *ibid.* 129, 190 (1963); R. T. Pu, Ph.D. thesis, University of California, Berkeley, 1963 (unpublished).

[54]R. J. Damburg and S. Geltman, Phys. Rev. Lett. 20, 485 (1968).

[55]D. G. Truhlar, J. K. Rice, S. Trajmar, and D. C. Cartwright, Chem. Phys. Lett. 9, 299 (1971); J. K. Rice, D. G. Truhlar, D. C. Cartwright, and S. Trajmar, Phys. Rev. A 5, 762 (1972).

[56]G. Csanak, H. S. Taylor, and D. N. Tripathy, J. Phys. B 6, 2040 (1973); G. Csanak and H. S. Taylor, *ibid.* 6, 2055 (1973); G. Csanak, H. S. Taylor, and B. S. Yarlagadda, J. Mol. Struct. 19, 205 (1973).

[57]I. E. McCarthy and M. R. C. McDowell, J. Phys. B 12, 3775 (1979).